

LARGE SCATTER IN X-RAY EMISSION AMONG ELLIPTICAL GALAXIES: CORRELATIONS WITH MASS OF HOST HALO

WILLIAM G. MATHEWS¹, FABRIZIO BRIGHENTI^{1,2}, ANDREAS FALTENBACHER¹, DAVID A. BUOTE³, PHILIP J. HUMPHREY³,
 FABIO GASTALDELLO³, & LUCA ZAPPACOSTA³

Draft version July 7, 2018

ABSTRACT

Optically similar elliptical galaxies have an enormous range of X-ray luminosities. We show that this range can be attributed to large variations in the dark halo mass M_{vir} determined from X-ray observations. The K-band luminosity of ellipticals varies with virial mass, $L_K \propto M_{vir}^{0.75 \pm 0.22}$, but with considerable scatter, probably due to the stochastic incidence of massive satellite galaxies that merge by dynamical friction to form group-centered ellipticals. Both the observed X-ray luminosity $L_x \propto M_{vir}^{2.4}$ and $L_x/L_K \propto M_{vir}^{1.6}$ are sufficiently sensitive to the virial mass to explain the wide variation observed in L_x among galaxies of similar L_K . The central galaxy supernova energy per particle of diffuse gas increases dramatically with decreasing virial mass and elliptical galaxies with the lowest X-ray luminosities (and M_{vir}) are easily explained by supernova-driven outflows.

Subject headings: X-rays: galaxies – galaxies: clusters: general – X-rays: galaxies: clusters – galaxies: cooling flows

1. INTRODUCTION AND BACKGROUND

In spite of their very regular optical properties, elliptical galaxies with similar optical luminosities have X-ray luminosities that range over more than two orders of magnitude. Many attempts to explain this huge scatter or to find observable properties that correlate with residuals in this scatter have been inconclusive (e.g. Eskridge, Fabbiano & Kim 1995a,b,c; Ellis & O’Sullivan 2006; Mathews & Brighenti 2003 for a review).

Figure 1 shows a plot of X-ray and K-band luminosities for elliptical galaxies taken from the catalog of Ellis & O’Sullivan (2006). Most of the X-ray emission is from diffuse hot gas although stellar emission from low mass X-ray binaries (LMXB) contributes in galaxies of the lowest L_x . While the lower envelope of the distribution is well-defined by the locus for stellar LMXB emission, X-ray images of these low- L_x elliptical galaxies also show definite evidence of diffuse gas emission (e.g. Sarazin et al. 2001). There is no apparent concentration of gas-free ellipticals along the LMXB locus, confirming the general prevalence of diffuse emission. Figure 1 includes only a few ram-stripped, low- L_x elliptical galaxies orbiting in massive clusters that have nevertheless retained a small mass of ~ 1 keV gas (e.g. Sun et al. 2004; 2005). Our interest here is not these strongly ram-stripped galaxies, but similar galaxies that are isolated or central galaxies in groups.

Using an early data set based on *Einstein*, ROSAT and ASCA observations, Mathews & Brighenti (1998a) showed that the radius of half-X-ray emission r_{effx} decreases systematically with decreasing L_x in Figure 1. It was demonstrated later that this correlation could be understood as a variation of the dark halo mass (Mathews

& Brighenti 1998b). In this paper we extend this idea using more recent data to show that the scatter in L_x is intimately related to stochastic and systematic variations of the virial mass M_{vir} of the dark halos that surround them. Galaxies with smaller M_{vir} necessarily have fewer baryons and lower L_x and we use simple galaxy plus halo models to show that this effect alone can explain at most about half of the total observed range in $\log L_x$. However, galaxies/groups with the lowest L_x require AGN or supernova-driven outflows.

2. CORRELATIONS AMONG L_X , L_K AND M_{VIR}

The virial mass of dark host halos around elliptical galaxies can be directly determined from radial temperature and density profiles in the hot gas, assuming hydrostatic equilibrium. The total mass based on *Chandra* and XMM images can be attributed to a combination of stellar and dark mass profiles. *Chandra* observations are particularly valuable since LMXB sources can be resolved and removed. The galaxy sample we consider here with known virial masses is shown in Figure 1 with filled symbols: squares are from Humphrey et al (2006), circles are from Gastaldello et al. (2006) and the hexagons are X-ray luminous galaxies tabulated in Mathews et al. (2005).

Figure 2a shows that M_{vir} for the sample galaxies increases with L_x according to the correlation

$$\log M_{vir} = -(4.20 \pm 0.92) + (0.42 \pm 0.02) \log L_x \quad (1)$$

(with correlation coefficient 0.75) indicated with a dashed line, i.e. $L_x \propto M_{vir}^{2.4}$. This and subsequent correlations are formal least square fits, assuming a mean typical error $\Delta \log M_{vir} = 0.090$ which is small compared to the intrinsic spread in the data. The quality of our least squares fit in Figure 2a is limited by the cosmic spread in M_{vir} , but it is consistent with a slightly steeper variation $M_{vir} \propto L_x^{0.65}$ in massive clusters found by Reiprich & Böhringer (2002).

Figure 2b indicates a very wide variation in the virial mass with K-band luminosity of the central galaxy L_K ,

¹ UCO/Lick Observatory, Dept. of Astronomy and Astrophysics, University of California, Santa Cruz, CA 95064

² Dipartimento di Astronomia, Università di Bologna, via Ranzani 1, Bologna 40127, Italy

³ Dept. of Physics & Astronomy, Univ. California Irvine, 4129 Fredrick Reines Hall, Irvine, CA 92697

superimposed on a positive M_{vir} - L_K correlation,

$$\log M_{vir} = -(1.75 \pm 1.04) + (1.34 \pm 0.09) \log L_K, \quad (2)$$

(dashed line in Fig 2b) with correlation coefficient 0.58.

The mean optical luminosity of group and cluster-centered elliptical galaxies is known to increase, then saturate as the virial mass of the cluster increases. Halo masses around elliptical galaxies in small groups can be determined from the SDSS galaxy-mass correlation function (Cooray and Milosavljevic 2005), from weak galaxy-galaxy lensing (Yang et al. 2003), and from the X-ray temperature of the gas (Lin & Mohr 2004). The L_K of the central galaxy varies as $M_{vir}^{0.85}$ for $M_{vir} \lesssim 10^{12} M_\odot$ and as $M_{vir}^{0.25}$ for $M_{vir} \gtrsim 10^{14.5} M_\odot$. The intermediate variation $L_K \propto M_{vir}^{0.75}$ in equation (2) is consistent with these results for the range in M_{vir} that we consider.

The scatter in Figure 2b arises because of an intrinsic (log-normal) cosmic variance of M_{vir} among galaxies of similar L_K . The central galaxy forms from a rather small number of luminous satellite galaxies that merge at the halo center because of dynamical friction (e.g. Faltenbacher & Mathews 2005). Since dynamical friction varies as the square of the ratio of the galaxy subhalo mass to the mass of the host halo, only the most luminous group satellite galaxies merge at the center. Therefore, because of the relative rarity and stochastic incidence of luminous satellite galaxies, halos of the same mass can have a range of L_K for the central elliptical (e.g. Cooray 2006). Conversely, halos of different M_{vir} can contain central galaxies with similar L_K , as seen in Figure 2b.

Figure 2c shows that the mean gas temperature $\langle kT \rangle$ (estimated from $T(r)$ profiles for the Humphrey et al 2006 data) is tightly correlated with the virial mass. The dashed line describing this correlation is given by

$$\log M_{vir} = (13.5 \pm 0.02) + (2.07 \pm 0.09) \log \langle kT \rangle. \quad (3)$$

This kT - M_{vir} correlation is similar to those found in clusters with more massive halos (Arnaud et al. 2005; Vikhlinin et al. 2006).

3. RELATION OF L_X TO BARYON CLOSURE

The physical origin of the vertical deviation of L_x in Figure 1 is best characterized by the logarithmic distance $D(\log L_x)$ of each galaxy from the (dash-dotted) locus of baryonic closure, the approximate L_x expected if the most massive dark halos for each L_K are filled with gas (and stars) containing the maximum baryonic mass allowed by the cosmic baryon ratio $f_b = \Omega_b/\Omega_m = 0.176$ observed by the *Wilkinson Microwave Anisotropy Probe* (WMAP; Spergel et al. 2006). If a galaxy/group is baryonically closed, no gas has been ejected from the confining halo by AGN or supernova energy. Since the total mass of diffuse gas can be reasonably well estimated in several of the most luminous groups in the sample, we know that at least some galaxies/groups with the largest L_x are quite close to the closure locus (Mathews et al. 2005),

$$(\log L_x)_{closure} \approx 18.361 + 2.18 \log L_K,$$

shown by the dash-dotted line in Figure 1. The deviation in L_x of a given galaxy below the closure locus is

$$D(\log L_x) = (\log L_x)_{closure} - \log L_x. \quad (4)$$

Figure 2d shows an anticorrelation between $D(\log L_x)$ and M_{vir}

$$\log M_{vir} = (14.01 \pm 0.03) - (0.34 \pm 0.03) D(\log L_x), \quad (5)$$

(dashed line in Fig. 2d), confirming that the virial mass is key to understanding the wide scatter in L_x among elliptical galaxies in Figure 1. Eliminating M_{vir} between equations (1) and (2), we derive the approximate direction in the L_x - L_K plane along which M_{vir} decreases most rapidly, shown by the short-dashed arrow in Fig. 1.

4. ISOTHERMAL MODELS

The closure locus in Figure 1 – the approximate maximum M_{vir} and L_x for galaxy/groups for each L_K – can be related to simple models for the hot gas. We assume that the gas is isothermal with $\langle kT \rangle$ given by equation (3) and in hydrostatic equilibrium in the potentials of the dark halo and central galaxy. The NFW halo is characterized by its virial mass M_{vir} (using a mean concentration $c(M_{vir})$ from Bullock et al. 2001). The virial radius is defined by an overdensity $\Delta = 104$ above the critical density $\rho_c = 9.24 \times 10^{-30} \text{ gm cm}^{-3}$. The central galaxy is assumed to have a de Vaucouleurs mass distribution described by L_K and effective radius $r_{eff} = 4.16(M_*/10^{11} M_\odot)^{0.56} \text{ kpc}$ (Boylan-Kolchin et al. 2005). The B-band stellar mass to light ratio is $\Upsilon_B = M_*/L_B = 7.5$ and we adopt $L_K/L_{K\odot} = 4.15L_B/L_{B\odot}$ appropriate for an old stellar population in elliptical galaxies (Ellis & O’Sullivan 2006). Solutions of these isothermal, hydrostatic models with $f_b = 0.176$ (and including gas self-gravity) give the maximum L_x within r_{vir} for any given M_{vir} and L_K . For each L_K we increase M_{vir} until L_x of the model exceeds all observed values and eventually recover the approximate closure locus described by Mathews et al. (2005) (dash-dotted line in Figure 1), given by $L_x = 2.19 \times 10^{42} (L_K/10^{11} L_{K\odot})^{2.18} \text{ erg s}^{-1}$. The closure locus empirically defines an upper limit to the L_x - L_K distribution and is consistent with the large baryon fractions $\approx f_b$ determined for well-observed galaxy/groups having the largest L_x/L_K . Since L_x of the models extend to r_{vir} while the observed L_x do not, even galaxies with the largest L_x in Figure 1 are expected to lie slightly below the closure locus.

In principle, galaxies that lie significantly below the closure line in Figure 1 could also be baryonically closed, i.e. with fixed $f_b = 0.176$, L_x is expected to decrease with M_{vir} . Although we view this possibility as highly unlikely, it is interesting to explore how much of the spread in Figure 1 can be understood with this extreme assumption of universal baryon closure. Consider simple models in which M_{vir} decreases below the closure locus in Figure 1, holding L_K of the central galaxy fixed and ignoring the stellar mass of satellite galaxies. For central galaxies of mass $M_* = \Upsilon_B L_B = (7.5/4.15)L_K M_\odot$ the fraction of baryons remaining in diffuse gas is

$$f_g = M_{gas}/M_{vir} = f_b - 1.8L_K/M_{vir}. \quad (6)$$

L_x declines with M_{vir} faster than M_{gas} since stars (with constant L_K) consume an increasingly larger fraction of the baryons in smaller halos. In this simple model, where mass loss from evolving stars is neglected, the mass of diffuse gas (and L_x) completely vanishes ($f_g = 0$) for halo masses less than $M_{vir,0} = 10.3L_K$.

Isothermal models with $\log L_K = 11.5$ and $\log(M_{vir}/M_\odot) = 13.5, 13$ and 12.6 (models *a, b*, and

c respectively) are listed in Table 1 and plotted in Figure 1. From equation (6) model c is close to the $f_g = 0$ limit. The X-ray luminosities of these models extend over nearly half the total spread in Figure 1. The radius r_{effx} in Table 1 that includes half of the total projected L_x decreases systematically with L_x , qualitatively confirming the correlation between the observed X-ray sizes and L_x found by Mathews & Brighenti (1998a). Also listed in Table 1 are the thermal and binding energies per gas particle, e_{th} and e_{bind} , as well as the corresponding energy released by supernovae of Type II, e_{II} , calculated assuming a Salpeter IMF, and Type Ia, e_{Ia} , estimated from the total iron mass produced by an old stellar population, $M_{Fe}/M_* \approx 0.0006$ (De Grandi et al. 2004), assuming $0.7 M_\odot$ in iron per supernova.

As M_{vir} decreases, the supernova energy in the central galaxy varies from relative insignificance for model a to dominance in model c where $e_{II} + e_{Ia} \gg e_{bind}$, the gravitational binding energy per gas particle. The global energetics in Table 1 strongly suggest that the remaining scatter in L_x in Figure 1 below model c can easily be explained by supernova-driven gaseous outflows from low M_{vir} halos. It is more likely that outflows reduce L_x for all galaxies in Figure 1, and that outflows are disproportionately effective as M_{vir} decreases with increasing $D(\log L_x)$ (Fig. 2d).

Another feature in the galaxy distribution in Figure 1 that remains to be understood is the absence of galaxies near the closure locus but with $\log L_K \lesssim 11.2$. If the halo mass decreases in the direction of the short-dashed arrow, it is plausible that the absence of galaxies in this region can also be understood in terms of supernova-driven outflows combined with a modest gas supply from evolving stars, maintaining L_x close to the LMXB lower limit.

Finally, we note another observable feature that correlates with M_{vir} : the shape of the radial gas temperature profile $T(r)$. Massive galaxy groups with large L_x have a temperature maximum displaced from the center, but in low- L_x ellipticals the temperature peaks at the center (e.g. Humphrey et al. 2004; Humphrey et al. 2006; O'Sullivan & Ponman 2004). The origin of this difference

in thermal profiles can be explained by the ratio of the mass of the galaxy to its host halo (Mathews & Brighenti 2003). When a group-centered elliptical resides in a more massive halo, the virial (and gas) temperature throughout most of the halo exceeds that of the central galaxy, resulting in a positive temperature gradient in the inner regions. However, when a similar elliptical has a halo of lower mass, the gas temperature peaks at the center where it approaches the virial temperature of the stellar bulge. This observed pattern is consistent with the expected variation of L_x with M_{vir} in Figures 1 and 2a.

5. CONCLUSIONS

Our main conclusions are:

- (1) The large variation of X-ray luminosity among group-centered elliptical galaxies of similar optical luminosity can be ascribed to a large cosmic variation in the surrounding dark halo mass.
- (2) For galaxies with similar L_K a significant fraction of the observed correlation between L_x and M_{vir} can be expected simply because smaller halos contain fewer baryons, less hot gas, and lower L_x . However, with decreasing M_{vir}/L_K supernova (or AGN) driven outflows become more likely, reducing L_x further.
- (3) M_{vir} decreases with both L_x and L_K in the L_x - L_K plot.
- (4) The upper envelope of elliptical galaxies in the L_x - L_K plot lies close to the locus of WMAP baryon closure for galaxies having the most massive dark halos at each L_K .
- (5) Previously found correlations between the X-ray luminosity of elliptical galaxies (having similar L_K) and their X-ray sizes (Mathews & Brighenti 1998a) or temperature profiles (Humphrey et al. 2006) are also consistent with a systematic decrease in halo mass for smaller L_x .

Studies of the evolution of hot gas in elliptical galaxies at UC Santa Cruz are supported by NASA grants NAG 5-8409 & ATP02-0122-0079 and NSF grant AST-0098351 for which we are very grateful.

REFERENCES

- Arnaud, M., Pointecouteau, E., & Pratt, G. W. 2006, *A&A*, 441, 893
- Boylan-Kolchin, M., Ma, C.-P., & Quataert, E. 2004, *ApJ*, 613, L37
- Bullock, J. et al. 2001, *MNRAS*, 321, 559
- Cappellaro, E., Evans, R., & Truratto, M. 1999, *A&A*, 350, 459
- Cooray, A. 2006, *MNRAS* (submitted) (astro-ph/0509033)
- Cooray, A. & Milosavljevic, M. 2005, *ApJ*, 627, L85
- De Grandi, S., Ettori, S. & Longhetti, M. 2004, *A&A*, 419, 7
- Ellis, S. C., & O'Sullivan, E. 2006, *MNRAS*, 367, 627
- Eskridge, P. B., Fabbiano, G. & Kim, D.-W. 1995a, *ApJS*, 97, 141
- Eskridge, P. B., Fabbiano, G. & Kim, D.-W. 1995b, *ApJ*, 442, 523
- Eskridge, P. B., Fabbiano, G. & Kim, D.-W. 1995c, *ApJ*, 448, 70
- Faltenbacher, A. & Mathews, W. G. 2005, *MNRAS*, 358, 139
- Gastaldello, F., Buote, D. A., Humphrey, P. J., Zappacosta, L., Bullock, J. S., Brighenti, F., Mathews, W. G. 2006, *ApJ* (submitted) (astro-ph/0610134)
- Humphrey, P. J., Buote, D. A., Gastaldello, F., Zappacosta, L., Bullock, J. S., Brighenti, F. & Mathews, W. G. 2006, *ApJ* (in press) (astro-ph/0601301)
- Humphrey, P. J., Buote, D. A. & Canizares, C. R. 2004, *ApJ*, 617, 1047
- Kim, D.-W. & Fabbiano, G. 2004, *ApJ*, 611, 846
- Kravtsov, A. V., Nagai, D., Vikhlinin, A. A. 2005, *ApJ*, 625, 588
- Lin, Y.-T. & Mohr, J. J. 2004, *ApJ*, 617, 879
- Lin, Y.-T., Mohr, J. J. & Stanford, S. A. 2003, *ApJ*, 591, 749
- Mathews, W. G., Faltenbacher, A., Brighenti, F. & Buote, D. A. 2005, *ApJ*, 634, L137
- Mathews, W. G. & Brighenti, F. 2003, *Ann. Rev. Astron. & Ap.* 41, 191
- Mathews, W. G. & Brighenti, F. 1998b, *ApJ*, 503, L15
- Mathews, W. G. & Brighenti, F. 1998a, *ApJ*, 493, L9
- O'Sullivan, E. & Ponman, T. J. 2004, *MNRAS*, 354, 935
- Reiprich, T. H. & Böhringer, H. 2002, *ApJ*, 567, 716
- Sarazin, C. L., Irwin, J. A. & Bregman, J. N. 2001, *ApJ*, 556, 533
- Spergel, D. N. et al. 2006, *ApJ* (submitted) (astro-ph/0603449)
- Sun, M., Jerius, D. & Jones, C. 2005, *ApJ*, 633, 165
- Sun, M., Forman, W., Vikhlinin, A., Hornstrup, A., Jones, C. & Murray, S. S. 2004, *ApJ*, 612, 805
- Vikhlinin, A. et al. 2006, *ApJ*, 640, 691
- Yang, X., Mo, H.-J., Kauffmann, G. & Chu, Y.-Q. 2003, *MNRAS*, 358, 217

TABLE 1
 ISOTHERMAL MODELS WITH
 $L_K = 10^{11.5}$

| model | <i>a</i> | <i>b</i> | <i>c</i> |
|-------------------------|----------|----------|----------|
| $\log M_{vir}(M_\odot)$ | 13.5 | 13.0 | 12.6 |
| $\log kT$ (keV) | 1.0 | 0.6 | 0.4 |
| $\log M_{gas}(M_\odot)$ | 12.66 | 12.07 | 11.11 |
| $\log L_x$ (erg/s) | 43.43 | 42.77 | 42.09 |
| r_{effx} (kpc) | 151 | 104 | 0.9 |
| e_{th} (keV/part) | 1.5 | 0.9 | 0.6 |
| e_{bind} (keV/part) | 2.3 | 1.1 | 0.6 |
| e_{II} (keV/part) | 0.4 | 1.5 | 14. |
| e_{Ia} (keV/part) | 0.03 | 0.1 | 1.2 |

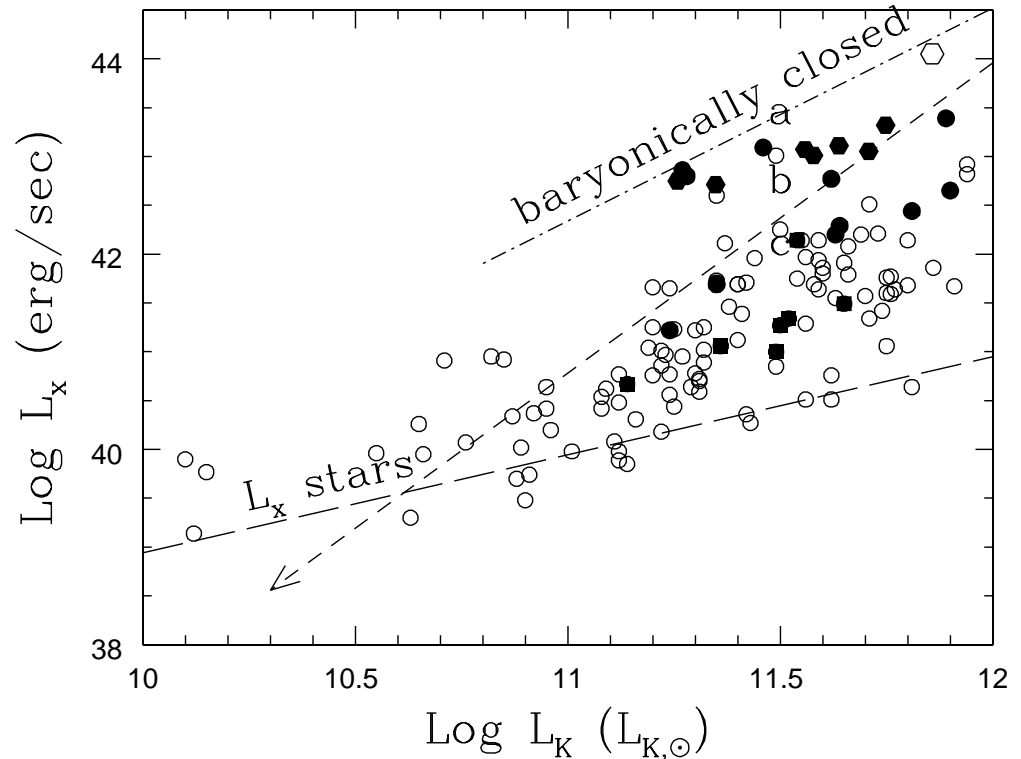


FIG. 1.— K-band and X-ray luminosities of X-ray-detected elliptical galaxies ($T < -4$) from the catalog of Ellis & O’Sullivan (2006). Filled squares, circles and hexagons are our sample galaxies for which the virial mass has been determined except RXJ146 (the open hexagon) which is useful to establish the upper envelope of the data. The lower long-dashed line shows the approximate emission from low mass X-ray binary stars (Kim & Fabbiano 2004). The upper dash-dotted line is the approximate locus of baryon closure (Mathews et al. 2005). The short-dashed arrow shows the direction in which M_{vir} decreases most rapidly. Labels *a*, *b* and *c* show locations of several baryonically closed, isothermal models listed in Table 1.

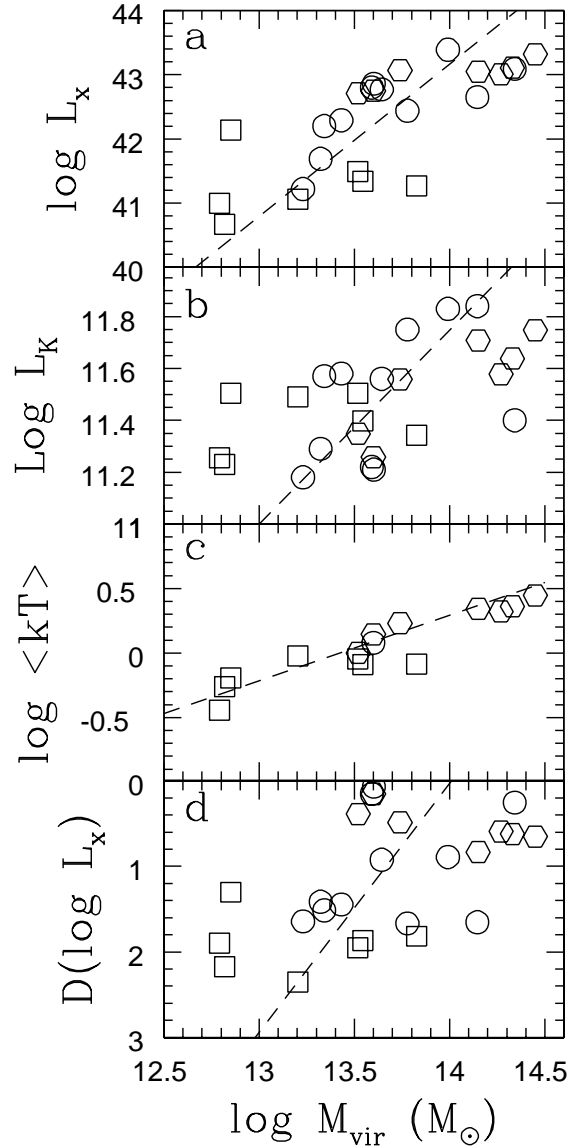


FIG. 2.— (a) Variation of X-ray luminosity L_x (in erg s^{-1}) of the sample galaxies with the virial mass (in M_{\odot}) of their host halos. (b) Variation of the central galaxy K-band luminosity (in $L_{K\odot}$) with virial mass. (c) Variation of mean gas temperature (in keV) with virial mass. (d) Variation of the logarithmic deviation from the locus of baryon closure in Figure 1 with the halo virial mass. Note that $D(\log L_x)$ increases downward, as in Figure 1. Dashed lines show correlations discussed in the text. Note that all correlations are apparent in published data from Humphrey et al (2006) (*open squares*) and Mathews et al. (2005) (*open hexagons*), while the data of Gastaldello et al. (2006) (*open circles*) fall in between.